Virioplankton and virus-induced mortality of prokaryotes in the Kara Sea (Arctic) in summer

Alexander Ivanovich Kopylov [Corresp., 1], Elena Anatoliyevna Zabotkina [1], Andrey Fiodorovich Sazhin [Corresp., 2], Nadezda Romanova [2], Nikolay Belyaev [2], Anastasia Drozdova [2]

[1] Papanin Institute for Biology of Inland Waters Russian Academy of Sciences, Borok, Yaroslavl region, Russia

[2] SHIRSHOV INSTITUTE OF OCEANOLOGY OF RUSSIAN ACADEMY OF SCIENCES, Moscow, Russia

Corresponding Authors: Alexander Ivanovich Kopylov, Andrey Fiodorovich Sazhin
Email address: kopylov@ibiw.ru, andreysazhin@yandex.ru

Among the Arctic seas, the largest volume of river runoff (~45% of the total river-water inflow into the Arctic Ocean) enters the Siberian Kara Sea. The viral communities of the Kara Sea are important for the functioning of the marine ecosystem. Studies of virus–prokaryote interactions on the Kara Sea shelf have been conducted only in spring and autumn. Here, we investigated the abundance of free viruses, viruses attached to prokaryotes, and pico-sized detrital particles; the morphology (shape and size) of the viruses, viral infection and virus-mediated mortality of prokaryotes in early summer, i.e., during a seasonal ice melting period and maximum inflow of river-water volumes with high concentrations of dissolved and suspended organic carbon. Seawater samples for microbial analyses were collected across the Kara Sea shelf zone on board the *Norilskiy Nickel* as a research platform from June 29 to July 15, 2018. Abundances of prokaryotes (range $(0.6–25.3) \times 10^5$ cells mL^{-1}) and free viruses (range $(10–117) \times 10^5$ viruses mL^{-1}) were correlated (r = 0.63, p = 0.005) with an average virus: prokaryote ratio of 23.9±5.3. The abundance of free viruses and viral-mediated mortality of prokaryotes were significantly higher in early summer than in early spring and autumn. Free viruses with a capsid diameter of 16−304 nm were recorded in the examined water samples. Waters in the Kara Sea shelf contained high concentrations of suspended organic particles 0.25−4.0 μm in size (range $(0.6–25.3) \times 10^5$ particles mL^{-1}). The proportions of free viruses, viruses attached to prokaryotes, and viruses attached to pico-sized detrital particles were 89.8±6.0%, 2.2±0.6% and 8.0±1.3%, respectively, of the total virioplankton abundance (on average $(61.5±6.2) \times 10^5$ viruses mL^{-1}). Viruses smaller than 60 nm clearly dominated at all studied sites. The majority of free viruses were not tailed. We estimated that an average of 1.4% (range 0.4–3.5%) of the prokaryote community was visibly infected by viruses, suggesting that a significant proportion of prokaryotic secondary production,

11.4% on average (range 4.0−34.0%), was lost due to viral lysis. There was a negative correlation between the abundance of pico-sized detrital particles and the frequency of visibly infected prokaryotic cells: r = -0.67, p = 0.0008.

1   **Virioplankton and virus-induced mortality of prokaryotes in the Kara Sea (Arctic) in**

2   **summer**

3   Alexander I. Kopylov[1][*], Elena A. Zabotkina[1], Andrey F. Sazhin[2][**], Nadezhda D. Romanova[2],

4   Nicolay A. Belyaev[2], Anastasia H. Drozdova[2]

5   *[1] Papanin Institute for Biology of Inland Waters Russian Academy of Sciences, Borok, Yaroslavl*

6   *oblast, Russia*

7   *[2] Shirshov Institute of Oceanology of Russian Academy of Sciences, Moscow, Russia*

9   Subjects: Ecology, Marine Biology, Hydrobiology, Microbiology

11   Corresponding author *: Alexander Kopylov

12   109, Borok, Nekouzsky district, Yaroslavl oblast, 152742, Russia

13   E-mail address: kopylov@ibiw.ru

14   Corresponding author **: Andrey Sazhin

15   36, Nakhimovskiy prospect, Moscow, 117997, Russia

16   E-mail address: andreysazhin@yandex.ru

18   **ABSTRACT**

19   Among the Arctic seas, the largest volume of river runoff (~45% of the total river-water inflow

20   into the Arctic Ocean) enters the Siberian Kara Sea. The viral communities of the Kara Sea are

21   important for the functioning of the marine ecosystem. Studies of virus–prokaryote interactions

22   on the Kara Sea shelf have been conducted only in spring and autumn. Here, we investigated the

23   abundance of free viruses, viruses attached to prokaryotes, and pico-sized detrital particles; the

24   morphology (shape and size) of the viruses, viral infection and virus-mediated mortality of

25   prokaryotes in early summer, i.e., during a seasonal ice melting period and maximum inflow of

26   river-water volumes with high concentrations of dissolved and suspended organic carbon.

27   Seawater samples for microbial analyses were collected across the Kara Sea shelf zone on board

28   the *Norilskiy Nickel* as a research platform from June 29 to July 15, 2018. Abundances of

29   prokaryotes (range $(0.6–25.3) \times 10^5$ cells mL^{-1}) and free viruses (range $(10–117) \times 10^5$ viruses

30   mL^{-1}) were correlated (r = 0.63, p = 0.005) with an average virus: prokaryote ratio of 23.9±5.3.

31   The abundance of free viruses and viral-mediated mortality of prokaryotes were significantly

32   higher in early summer than in early spring and autumn. Free viruses with a capsid diameter of

33   16−304 nm were recorded in the examined water samples. Waters in the Kara Sea shelf

34   contained high concentrations of suspended organic particles 0.25−4.0 μm in size (range (0.6–

35   25.3) $\times$ 10^5 particles mL^{-1}). The proportions of free viruses, viruses attached to prokaryotes, and

36   viruses attached to pico-sized detrital particles were 89.8±6.0%, 2.2±0.6% and 8.0±1.3%,

37   respectively, of the total virioplankton abundance (on average (61.5±6.2) $\times$ 10^5 viruses mL^{-1}).

38   Viruses smaller than 60 nm clearly dominated at all studied sites. The majority of free viruses

39   were not tailed. We estimated that an average of 1.4% (range 0.4–3.5%) of the prokaryote

40   community was visibly infected by viruses, suggesting that a significant proportion of

41   prokaryotic secondary production, 11.4% on average (range 4.0−34.0%), was lost due to viral

42   lysis. There was a negative correlation between the abundance of pico-sized detrital particles and

43   the frequency of visibly infected prokaryotic cells: r = -0.67, p = 0.0008.

45   **LIST OF ABBREVIATIONS**

47   *PD* – pico-sized detrital particles

48   N_{PD} – abundance of pico-sized detrital particles

49   N_{PDV} – abundance of pico-sized detrital particles with attached viruses

50   N_{PR} – abundance of prokaryotes

51   N_{PRV} – abundance of prokaryotes with attached viruses

52   V_{PR} – volume of prokaryotic cell

53   B_{PR} – biomass of prokaryotes

54   N_{VF} – abundance of free viruses

55   VPR – virus : prokaryote ratio

56   N_{VPR} – abundance of viruses attached to prokaryotic cells

57   N_{VPD} – abundance of viruses attached to pico-sized detrital particles

58   D_{VF} – capsid diameter of free viruses

59   *FVIC* – frequency of visibly infected prokaryotic cells

60   N_{PRVIC} – abundance of visibly infected prokaryotic cells

61   *FIC* – frequency of infected prokaryotic cells

62   *VMPR* – viral-mediated mortality of prokaryotes

63   *BS* – burst size

64

65   **INTRODUCTION**

66

67   Studies conducted in different Arctic regions have demonstrated that viruses constitute the most

68   abundant component of the plankton community and play a significant role in the functioning of

69   cold-water microbial communities, as well as in marine communities in temperate and tropical

70   climates (Middelboe, Nielsen & Bjørnsen, 2002; Hodges et al., 2005; Wells & Deming, 2006a;

71   Suttle, 2007; Maranger et al., 2015; Sandaa et al., 2018). In polar regions viruses maintain their

72   infectivity at low temperatures (Middelboe, Nielsen & Bjørnsen, 2002; Weinbauer, Brettar &

73   Höfle, 2003), and viral lysis can be important in controlling prokaryotic abundance (Guixa-

74   Boixereu et al., 2002; Wells & Deming, 2006b). Viral lysis of prokaryotes may also influence

75   the composition of the prokaryotic community (Weinbauer & Rassoulzadegan, 2004) and trigger

76   the release of intracellular material upon lyses, which in turn stimulates the cycling of dissolved

77   organic carbon (DOC) by heterotrophic prokaryotes (Bratbak, Thingstad & Heldal, 1994;

78   Wilhelm & Suttle, 1999; Suttle, 2007). Coastal marine systems in the Arctic typically contain

79   high concentrations of inorganic and organic particles, which enter the water column via melting

80   of land and sea ice and runoff from large rivers (Lasareva et al., 2019; Maat, Prins & Brussaard,

81   2019). The high suspended particle load may substantially reduce the ability of viruses to infect

82   prokaryotes as viruses are efficiently adsorbed by silt, clay, and organic particles (Murray &

83   Jackson, 1992; Simon et al., 2002).

84   The Kara Sea is a heterogeneous and productive marine ecosystem within the Arctic Ocean,

85   which plays a key role in the carbon cycle. The Kara Sea is mostly a shallow Arctic shelf basin

86   influenced by river runoff: it receives 1300–1400 km^3 of fresh water annually, accounting for

87   41% of total freshwater runoff to the Arctic Ocean (Makkaveev et al., 2015).

88   Knowledge of the patterns of the transformation of organic matter and remineralization of

89   nutrients in the low water-temperature conditions on the Kara Sea shelf in the modern period

90   demand detailed information on the structural and functional organization of microbial

91   communities. These data are also necessary to assess possible future changes in the structure and

92   functioning of prokaryotic and viral communities in the process of global warming, increased

93 runoff from Siberian rivers flowing into the Arctic regions, and increasing anthropogenic load on
94 the Kara Sea shelf.

95

96 In recent years, data have been obtained on the abundance of planktonic prokaryotes and viruses
97 and virus-mediated mortality of prokaryotes in different areas of the Kara Sea shelf in early
98 spring and autumn (Kopylov et al., 2015, 2019). However, virioplankton and viral infections of
99 heterotrophic prokaryotes in the Kara Sea in the phenological period of early summer remain
100 unstudied.
101 A specific feature of this phenological period between spring and summer is that planktonic
102 microbial communities in the western part of the sea function under melting land and sea ice
103 conditions, whereas in the eastern part, under conditions of maximum inflow of water masses of
104 the Ob and Yenisei rivers, which alter the salinity regime of this water area and transport a large
105 amount of mineral and organic matter. The river runoff of the Siberian rivers has a pronounced
106 seasonality. In May-June, the Ob River brings 136 km^3 of fresh water or 32% of the total annual
107 river flow to the Kara Sea, and the Yenisei River – 284 km^3 or 45% of its annual river flow.
108 During these two months, 1.338×10^9 g of dissolved organic carbon (*DOC*) or 32% of the annual
109 *DOC* input enters the Kara Sea from the Ob River, 2.942×10^9 g *DOC* or 63% of the annual
110 *DOC* input from the Yenisei River (Holmes et al., 2002). Accordingly, during this period, a
111 much larger amount of dissolved *DOC* and biogenic elements enters the sea compared to other
112 seasons (Holmes et al., 2002). Higher *DOC* concentrations and a relatively high water
113 temperature, apparently, should contribute to a more intensive reproduction of heterotrophic
114 bacteria and, accordingly, a greater activity of their obligate parasites – bacteriophage viruses".
115 The allochthonous dissolved and suspended organic matter entering the Kara Sea has a
116 significant impact both on the functioning of prokaryotes and the structure and activity of viruses
117 (Kopylov et al., 2022). The results obtained in this research can be used to fill the
118 прокариотinformation gap on the state of planktonic prokaryotes and viruses during early
119 summer and thereby reconstruct the seasonal cycle of the planktonic microbial community in this
120 section of the Arctic shelf. Emerging data suggest that the planktonic microbial assemblages in
121 the Kara Sea are active and diverse and can respond rapidly to changes in environmental
122 conditions (Kopylov et al., 2017; Romanova & Boltenkova, 2020; Romanova et al., 2022).

123 Based on this research, we test the hypothesis that the abundance of free viruses is maximal in

124 early summer, and not in other seasons: in spring; in midsummer, when the Ob and Yenisei

125 floods end; or later, during the autumn flood of the rivers. We also assume that viral infection

126 and virus-mediated mortality of prokaryotes is higher than in other seasons.

127 This determined the aim of our investigation, to assess for the first time the abundance and

128 activity of planktonic viruses in the Kara Sea in early summer. The specific objectives were to

129 determine (1) the abundance of free viruses and viruses attached to prokaryotic cells and pico-

130 sized detrital particles, (2) morphological characteristics and capsid sizes of viral particles, (3)

131 frequency of visibly infected cells and virus-mediated mortality of prokaryotes, and (4)

132 significance of the relationship between viruses and abiotic and biotic variables.

133

134 **MATERIALS & METHODS**

135

136 **Study sites and sampling**

137

138 Water samples were collected from June 29 to July 15, 2018, on board the *Norilskiy Nickel* at 21

139 stations along the vessel's course, from the station in the Barents Sea near the Kara Strait to the

140 one near the Taimyr Peninsula in the Yenisei estuary. Stations were located the Marine Area

141 (MA), a part of the shelf that receives no river runoff, and the Coastal Area (CA), adjacent to the

142 Ob and Yenisei estuaries (Fig. 1). Samples at stations 3 and 4 were taken in ship-made channels

143 in an ice-covered water area; stations 5, 24, and 25 were located in open water among ice fields.

144 Other stations were ice-free.

145 Temperature was measured with an SBE-39 probe and LCD thermometer (HANNA Checktemp-

146 1). Salinity (in practical salinity units) was measured with a Kelilong PHT-028 salinity meter

147 (China). Surface water samples (depth 0.5 m) for biological variables and dissolved organic

148 carbon (*DOC*) were collected by hand with a sterile 10-L bucket from the side of the ship. The

149 10-L buckets were rinsed with 0.1 M HCL prior to each DOC sampling. The DOC

150 concentrations were measured with a Shimadzu TOC-Vcph carbon analyzer coupled with an

151 SSM-5000A solid sample module (Belyaev, Peresypkin & Ponyaev, 2010).

152 Immediately after collection, water samples for microscopic studies were fixed with 25%

153 glutaraldehyde (final concentration 1%). Samples for determining the abundance and biomass of

154   prokaryotes were stored in sterile vials in the dark at 2−4°C until completion of work at the

155   station, no more than 1 h. After that, slides for epifluorescent microscopy were prepared and

156   stored at –24ºC for 1 month before analysis.

157   Samples for studying viruses were subsequently stored at –80ºC until processing at an office

158   laboratory.

159

160   **Enumeration of prokaryotes and smallest organic particles**

161

162   The abundances of prokaryotes (cocci and ellipsoids, rods and vibrios, and filaments were

163   estimated separately) were determined by standard techniques using fluorochrome 4', 6'–

164   diamidino–2–phenylindole (DAPI) and epifluorescence microscopy (Porter & Feig, 1980). From

165   each station, a 7-mL sample was stained with DAPI at a final concentration of 1 µg mL^{-1} and

166   filtered onto a black nuclepore filter (pore size 0.2 µm). Filters were placed on glass slides and

167   covered with Leica Type N immersion liquid and a cover glass.

168   Observation and counts were done under an epifluorescence microscope (Leica DM 5000 B) at a

169   magnification of ×1000 in two replicates. On each filter, at least 400 prokaryotes were counted

170   and the dimensions of at least 100 cells were measured. The wet biomass was estimated based on

171   the individual cell volume using Image Scope Color, version Image Scope M 2009, FEI Electron

172   Optics B.V. The carbon content in prokaryotic cells (C, fg C cells^{-1}) was calculated by the

173   following allometric equation: $C = 120 \times V^{0.72}$, where V is the mean volume of prokaryotic cells,

174   µm^3 (Norland, 1993).

175   Yellow pico-sized organic particles (0.25–4.0 µm in size), clearly distinguished from prokaryotic

176   cells, were also counted on DAPI-stained filters by epifluorescence microscopy (Porter & Feig,

177   1980; Mostajir, Dolan & Rassoulzadegan, 1995; Wells & Deming, 2003). On each filter, at least

178   400 pico-sized detrital particles were counted. The specific gravity of detritus particles was

179   assumed to equal to 1.

180

181   **Enumeration of viruses**

182

183   The viral particles were counted under an epifluorescence microscope using SYBR Green I

184   fluorochrome and Whatman Anodisc aluminum oxide membrane filters (pore size 0.02 µm)

185 (Noble & Fuhrman, 1998). Depending on the viral abundance, between 0.2 and 1.0 mL of water

186 was filtered onto the Anodisc filters. Counts were done under an Olympus BX51 epifluorescence

187 microscope (Olympus, Japan) using imaging Software cell^F (Olympus cell* Family, Olympus

188 Soft Imaging Solutions GMBH, Germany) at ×1000 magnification. For each water sample, two

189 filters were analyzed; counts yielded a minimum of 800 viruses. The carbon content in viral

190 particles was taken as 0.055 fg C virus^{-1} (Steward et al., 2007).

191

192 Viruses were also enumerated using transmission electron microscopy as described earlier

193 (Suttle, 1993; Brum, Schenck & Sullivan, 2013). In glutaraldehyde-fixed samples, viruses,

194 prokaryotes and smallest detrital particles contained in 50-mL samples were harvested by

195 centrifugation onto Pioloform (SPI, USA) and carbon-coated 400-mesh nickel grids, using an

196 OPTIMA L-90k ultracentrifuge (Beckman Coulter, USA) at 100 000 × g for 2 h. Two grids were

197 thus prepared for each water sample.

198 The grids were then positively stained for 30 s at room temperature with 1% (wt/vol) solutions of

199 uranyl acetate and lead citrate, and rinsed three times with deionized distilled water. The grids

200 were further analyzed under a JEM 1011 electron microscope (Jeol, Japan) at ×50 000–150 000

201 magnification.

202

203 Viruses were identified on the basis of morphology (round or hexagonal capsid structures, tailed

204 and nontailed), size and staining characteristics. Viruses were classified as myoviruses,

205 podoviruses, siphoviruses or icosahedral nontailed viruses (referred to as nontailed viruses

206 hereafter) based on their morphology as defined by the International Committee on Taxonomy of

207 Viruses (King et al., 2012). The following six classes of virus capsid size were examined to

208 characterize viral populations: <40, 40−60, >60−100, >100−150, >150−200, and >200 nm. No

209 less than 300 viral particles were analyzed per sample.

210 Transmission electron microscopy was used to measure the proportion of prokaryotic cells with

211 attached viruses, the proportion of smallest detrital particles (0.25−4.0 μm) with attached viruses,

212 and the abundance of viruses attached to a single prokaryotic cell and to a single detrital particle.

213 No less than 800 detrital particles were analyzed per sample.

214

215 **Virally infected prokaryotes and subsequent mortality**

216

217 The method of transmission electron microscopy was used to estimate the frequency of visibly

218 infected cells (*FVIC*, estimated as the share (%) of total prokaryotic abundance) and the mean

219 number of fully matured phages in prokaryotes (i.e., burst size (*BS*), viruses cell^{-1}) (Weinbauer,

220 2004). At least 1200 prokaryotic cells per sample were examined to determine *FVIC*.

221 Because viruses inside prokaryotic cells become visible during the last ~10% of the lytic cycle

222 (Proctor, Okubo & Fuhrman, 1993), FVIC were converted to the frequency of infected

223 prokaryotes (*FIC*) using the equation: $FIC = 7.1 \times FVIC - 22.5 \times FVIC^2$ (with data given as

224 percentages) (Binder, 1999). Virus-induced mortality of prokaryotes (VMPR, expressed as a

225 percentage of the production of prokaryotes,) was estimated from FIC following the model of

226 (Binder, 1999) with $VMPR = (FIC + 0.6 \times FIC^2)/ (1 - 1.2 \times FIC)$ and is given as a percentage. In

227 this model, it is assumed that in a steady system, infected and uninfected prokaryotes are grazed

228 at the same rate and that the latent period is equal to the prokaryotic generation time (Proctor,

229 Okubo & Fuhrman, 1993; Middelboe, 2000).

230

231 **Statistical analyses**

232

233 Correlations between the parameters were analyzed using Spearman's correlation coefficient

234 calculated by Past 4.03 software (Hammer, Harper & Ryan, 2001) with regard for the

235 prerequisites for the analyzed data.

236

237 **RESULTS**

238

239 **Environmental Parameters**

240

241 Table 1 shows values of the physical and chemical variables of the different surface seawater

242 samples collected at stations in the Barents Sea, Kara Strait, and the Marine and Coastal areas of

243 the Kara Sea. The water temperature and *DOC* values, on average for the area, were 2.7 and 3.7

244 times, respectively, higher in the CA than in the MA. At the same time, the average salinity and

245 alkalinity values were 2.8 and 1.7 times lower in the CA than in the MA, respectively (Fig. 2).

246 CA affected by the Ob and Yenisei runoff was also characterized by higher nutrient

247 concentrations and abundance of detrital particles with a size of 0.25–4.0 μm (Fig. 2).The

248 minimum and maximum chl a concentrations differed 150-fold in the Kara Sea (Table 1). The

249 chl a concentration was twice as high in the CA than in the MA (Fig. 2). The chl a and nutrient

250 concentrations were used to estimate the trophic conditions (Primpas & Karydis, 2011).

251 Oligotrophic conditions were found most studied stations in the MA. The chl a and nutrient

252 concentrations in the CA corresponded to oligo-mesotrophic waters.

253

254 **Abundance of prokaryotes and pico-sized organic particles**

255

256 The abundance (N_{PR}), average cell volume of prokaryotes, and biomass (B_{PR}) of prokaryotes

257 varied widely in the surface water layer (Table 2). The minimum and maximum N_{PR} and B_{PR}

258 values differed by 39 and 34 times across the transect, respectively. The highest values were

259 recorded in the eastern part of the CA (stations 12, 18). The average cell volume of prokaryotes

260 was 0.034 μm^3 in the Barents Sea, 0.042 μm^{-3} in the Kara Strait, 0.049±0.004 μm^3 in MA, and

261 0.035±0.002 μm^3 in CA.

262 As a result, over the entire period (June 29–July 15), N_{PR} and B_{PR} were on average 7.6 × 10^5 cells

263 mL^{-1} and 7.82 mg C m^{-3} in the Barents Sea, 1.8±0.4 × 10^5 cells mL^{-1} and 2.36±0.38 mg C m^{-3} in

264 MA, and 11.4±2.4 × 10^3 cells mL^{-1} and 12.15±2.60 mg C m^3 in CA.

265 For the overall data set, N_{PR} was positively correlated with T, Si, DOC, and chl a, but negatively

266 with S and Alk. There were no significant correlations between N_{PR} and (NO$_2$+NO$_3$), PO$_4$, N_{PD}.

267

268 The amount of pico-sized organic particles was high in the studied waters. These yellow particles

269 are pico-sized detritus (Mostajir, Dolan & Rassoulzadegan, 1995; Wells & Deming, 2003). The

270 abundance of detrital particles 0.25−4.00 μm (N_{PD}) in size varied between 1.75 and 20.59 ×10^5

271 particles mL^{-1}, and the wet weight, from 0.2 to 2.7 mg L^{-1} (Table 1). The average N_{PD} value in

272 the MA was lower than in the CA by 1.4 times, and the wet weight was 3.2 times lower (Fig. 2).

273

274 **Abundance of virioplankton and composition**

275

276 The epifluorescence microscopy estimates of free viral concentrations (N_{VF}) ranged from 10 ×10^5

277 viruses mL^{-1} to 11.7 ×10^6 viruses mL^{-1} (Fig.3, Table 3). The N_{VF} values in the Barents Sea and

278   the Kara Strait were lower than in the MA and CA (Fig. 4). The abundance N_{VF} in the Kara sea

279   was on average 58.6±5.7 ×10^5 viruses mL^{-1}. The virus : prokaryote ratio (*VPR*) in MA, on

280   average 37.0±7.2, was significantly higher than in the CA, on average 7.6±1.7 (Fig. 4). As a

281   result, the average *VPR* value on the Kara Sea shelf was 23.9±5.3.

282   For the overall data set, N_{VF} was positively correlated only with N_{PR} and *DOC* and negatively

283   with S (Table 4). Negative correlations were found between *VPR*, N_{PR}, *T*, and *DOC* (Table 4).

284

285   For the 6300 viruses and 21 samples examined, only four viral morphotypes were observed:

286   myoviruses (morphotypes with contractile tails of various shape), siphoviruses (morphotypes

287   with long noncontractile, often flexible tails), podoviruses (morphotypes with short tails), and

288   nontailed viruses (Fig. 3). Nontailed viruses dominated at all stations (57.0–82.0%), while

289   podoviruses, myoviruses, and siphoviruses were the next most abundant morphotypes, in that

290   order. The proportion of podoviruses was similar for all sites (17.3–17.9%).

291   The proportion of nontailed viruses out of the total viruses observed in the CA (65.9±1.9%) was

292   lower than in the MA (72.6±2.0%); conversely, the proportions of myoviruses and siphoviruses

293   out of the total viruses observed in the eastern Kara Sea were higher than those in the western,

294   1.6 and 2.6 times, respectively (Fig. 5).

295

296   The capsid diameter (D_{VF}) of free viral particles varied from 16 to 304 nm (Table 3). The

297   average capsid diameter varied between 37 and 64 nm per water sample, averaging 50±7 nm for

298   the 21 samples. The average D_{VF} values in the MA and CA were close, 53±2 and 51±2 nm,

299   respectively. On the Kara Sea shelf, the proportion of viruses with sizes of <40, 40−60,

300   >60−100, >100−150, >150−200, and >200 nm out of the total virioplankton abundance was, on

301   average, 40.54±14.85, 36.89±6.21, 18.67±10.26, 3.11±2.71, 0.64±1.09 and 0.15±0.37%,

302   respectively, for all water samples. Thus, from June 29 to July 15, 2018, viruses with a capsid

303   diameter of ≤60 nm amounted to 77.43% of the total abundance of free viruses.

304   The abundance of prokaryotes with viruses attached to their cells (N_{PRV}) varied from 0.2 × 10^5

305   cells mL^{-1} to 11.2 × 10^5 cells mL^{-1}, on average 1.6±0.5 × 10^5 cells mL^{-1}, which was 10.9–40.7%,

306   on average 24.0±1.4%, of the total abundance of prokaryotes (Fig. 3, Table 5). There were from

307   one to 12 viral particles attached to the surface of a cell of prokaryotes. From 1.2±0.1 to 1.9±0.3

308   viruses cell^{-1} were on the surface of a bacterial cell on average per water sample. The abundance

309   of viruses attached to prokaryotes (N_{VPR}) varied between 0.1×10^5 and 10.3×10^5 viruses mL^{-1},

310   averaging $(1.6\pm0.1) \times 10^5$ viruses mL^{-1}. The average N_{VPR} value in the CA was seven times

311   higher than in the MA (Fig. 4). The capsid diameter of viruses attached to prokaryotes varied

312   from 16 to 167 nm. The average capsid diameters of viruses attached to prokaryotes per water

313   sample varied between 45 and 88 nm, averaging 61±0.4 nm for all samples (Table 5).

314   The abundance of pico-sized detrital particles with attached viruses (N_{PDV}) ranged between 0.7

315      $\times 10^5$ to 4.2×10^5 particles mL^{-1} (on average $2.0\pm0.2 \times 10^5$ particles mL^{-1}) and was from 7.1 to

316   75.0% (on average 28.6±3.5%) of N_{PD} (Fig. 3, Table 6). The average amount of N_{PDV} in the

317   Barents Sea and in the MA was two- and 1.4-fold lower than in CA, respectively. From one to 17

318   viruses were attached to the surface of a single detrital particle. As a result, the abundance of

319   viruses attached to detrital particles (N_{VPD}) in the Kara Sea was, on average, $5.4\pm0.8 \times 10^5$

320   viruses mL^{-1}. The average abundances N_{VPD} in the Barents Sea and in the MA were 3.4 and 2.0

321   times lower than in the CA, respectively. The capsid diameter of viruses attached to detrital

322   particles ranged from 21 to137 nm. The average capsid diameters of viruses attached to PD

323   (pico-sized detrital particles) per water sample were 25−72 nm, averaging 56±3 nm for all

324   samples (Table 6).

325   As a result, the total abundance of virioplankton (N_{VT}) was $(14–140) \times 10^5$ viruses mL^{-1},

326   averaging $62\pm6 \times 10^5$ viruses mL^{-1}. Thus, the proportion of free viruses in N_{VT} was 72.0−98.1

327   (on average 89.8±6.0) % and was significantly higher than the proportion of viruses attached to

328   prokaryotes, 0.3−7.6 (on average 2.2±0.6) % and viruses attached to detrital particles 1.6−26.5

329   (on average 8.0±1.3) %. The largest contribution of free viruses to the formation N_{VT} was found

330   at station 3 in the MA; viruses attached to prokaryotic cells, at station 12 in the CA; and viruses

331   attached to detrital particles, at station 23 in the CA.

332   The total biomass of virioplankton (B_{VT}) varied between 0.08 and 0.77 mg C m^{-3}, averaging

333   0.33±0.03 mg C m^{-3}, and the proportion of virioplankton biomass of the prokaryotic biomass

334   (B_{VT}/B_{PR}) varied between 2.1 and 35.0% (on average 10.1±1.9%). The B_{VT} and B_{VT}/B_{PR} values

335   were, on average, 0.22 mg C m^{-3} and 3.2% in the Barents Sea; 0.11 mg C m^{-3} and 12.6% in the

336   Kara Strait; 0.30±0.03 mg C m^{-3} and 15.4±0.9% in the MA; 0.43±0.06 mg C m^{-3} and 4.2±0.3% in

337   the CA.

338

339   **Viral infection and virus-mediated mortality of prokaryotes**

340

341   The frequency of visibly infected prokaryotic cells ($FVIC$) in the Kara Sea ranged from 0.4 to

342   3.5% N_{PR}, averaging 1.3±0.2% N_{PR} (Fig. 3, Table 7). The average $FVIC$ values in the MA and

343   CA were close or slightly less than those in the Kara Strait and Barents Sea (Fig. 4). There was

344   no significant positive correlation between N_{PR} and $FVIC$. A negative correlation was found

345   between the abundance of N_{PD} and $FVIC$ (Table 4).

346

347   Calculations based on the $FVIC$ estimates showed that the proportion of virus-infected cells of

348   N_{PR} (FIC) varied from 2.9 to 22.1% of N_{PR} (on average 9.2±0.9% of N_{PR}), and the viral-mediated

349   mortality of prokaryotes ($VMPR$) was 4.0−34.0% (on average 11.4±1.5%) of the prokaryotic

350   production. The abundance of visibly infected prokaryotic cells (N_{PRVIC}) was (1−36) × 10^3 cells

351   mL^{-1}, on average, 8±2 × 10^3 cells mL^{-1}. The minimum and maximum N_{PRVIC} / N_{PRV} ratios differed

352   by seven times (Table 7) and the N_{PRV} / N_{PRVIC} ratio varied from 8 to 58. A strong positive

353   correlation was found between N_{PRV} and $N_{PRVIC,}$ $r = 0.89$, $p < 0.005$, $n = 21$. Whereas the average

354   abundance of viral infected prokaryotic cells in the MA was six times lower than in the CA, the

355   N_{PRVIC} / N_{PRV} values in these areas did not differ significantly, 5.8±1.0 and 4.9±1.1%,

356   respectively.

357   The number of phages in viral-infected prokaryotic cells (BS) fluctuated from 4 to 35 phages

358   cell^{-1}, averaging 7.1±0.7 phages cell^{-1} (Table 7).

359   Cocci+ellipsoid cells (58–71%) made the main contribution to the total abundance of

360   prokaryotes; rods and vibrios (28−41%) and filaments (0−3.0%) were less abundant (Fig. 6).

361   Rods and vibrios accounted for the largest fraction of virus-infected prokaryotes (69–94% of the

362   total abundance of infected prokaryotes), with lower numbers observed for cocci, ellipsoids, and

363   filaments (6−28% and 0–3%) (Fig. 6). That is, the phages infected prokaryotic cells of different

364   morphology at a different rate. The proportion of virus-infected rods and vibrios in the total

365   abundance of prokaryotes with the corresponding morphology was highest in the Barents Sea.

366   The proportion of virus-infected cocci and ellipsoids in the total abundance of prokaryotes with

367   the corresponding morphology was lowest in the CA.

368   Percentage of infected cells to the number of cocci and ellipsoids in the MA was higher than in

369   the CA, but the percentage of infected cells to the number of cocci and ellipsoids in the MA was

370   lower than in the CA (Fig. 6).

371

DISCUSSION

373

Abundance and biomass of viruses

375

376 In the current study, a high abundance of free viruses (N_{VF}) was detected in the Kara Sea in early

377 summer. N_{VF} consistently correlated with the abundance of prokaryotes (N_{PR}), whereas other

378 physical, chemical, and biological parameters correlated only weakly or not at all with N_{VF}.

379 Other researchers have also observed that virus-like particles were significantly correlated with

380 bacterial abundance, but correlations with other physicochemical or biological parameters were

381 insignificant (Stopar et al., 2003). The typical viral life cycles (lytic and lysogenic) and

382 replication rates are closely linked with host metabolism. Consequently, the factors regulating

383 the physiology of the host, as well as its production and removal are also important in governing

384 virus dynamics (Mojica, Brussaard, 2014; Zhang et al., 2021). A strong positive correlations

385 between N_{VF} and N_{PR} suggest that a significant amount of bacteriophages are present in the

386 virioplankton (Steward, Smith & Azam, 1996; Wommack & Colvell, 2000; Auguet et al., 2005).

387

388 Comparison of the results of studies of planktonic free viruses on the Kara Sea shelf conducted at

389 different times of the year showed that in in early summer, the average N_{VF} $58.6\pm5.7 \times 10^5$

390 viruses mL^{-1} and VPR 23.9 ± 4.9 values (present study) were higher than those obtained in early

391 spring, $10.8\pm0.2 \times 10^5$ viruses mL^{-1} and 6.9 ± 0.8 (Kopylov et al., 2019) and in autumn, 17.3 ± 0.8

392 $\times 10^5$ viruses mL^{-1} and 5.0 ± 0.5 (Kopylov et al., 2015; Kopylov et al., 2017). The N_{VF} in the Kara

393 Sea are within the range of N_{VF} $((0.1{-}64.1) \times 10^6$ viruses mL^{-1} and VPR $0.8{-}70.0\%$ values

394 recorded in the central Arctic Ocean and other Arctic seas (Steward, Smith & Azam, 1996;

395 Hodges et al., 2005; Steward et al., 2007; Clasen et al., 2008; Venger et al., 2016). In early

396 summer, in Kara Strait and Kara Sea of viral biomass (B_V) was $10.7\pm4.7\%$ of prokaryotic

397 biomass (B_{PR}) (present study). In early spring, the $B_V : B_{PR}$ ratio was significantly lower,

398 $2.2\pm1.3\%$ (Kopylov et al., 2019). For comparison, the viral biomass in the central Arctic Ocean

399 was about 6% of the prokaryotic biomass (Steward et al., 2007).

400

401 Morphological characteristics

402

403 Only four morphotypes (myoviruses, siphoviruses, podoviruses, and nontailed viruses) were

404 observed in this study, indicating that other morphotypes (for example, lemon-shaped or

405 filamentous) made up <1% of these marine viral assemblages. Nontailed viruses appear to

406 dominate numerically in the Kara Sea, since they constituted, on average, 65.9–72.6% of the

407 viral particles observed. Similar to the results obtained in other marine habitats (Stopar et al.,

408 2003; Auguet, Montanie & Lebaron, 2006), Brum, Schenck & Sullivan (2013) found that

409 nontailed icosahedral viruses dominate in the upper water column of the global oceans, making

410 up 51–92% of viral assemblages.

411 The majority of pelagic viruses in this study were less than 60 nm in diameter. Similar results

412 were reported for estuarine and marine waters at different latitudes (Bergh et al., 1989; Cochlan

413 et al., 1993; Weinbauer & Peduzzi, 1994; Alonso et al., 2001; Auguet, Montanie & Lebaron,

414 2006). In Kara Sea waters, the capsid size of viruses attached to prokaryotic cells rarely

415 exceeded 100 nm, 61±2 nm on average. Viruses of eukaryotic algae typically have a larger

416 capsid size (100–180 nm, on average 152 nm) (Van Etten, Lane & Meints, 1991), whereas the

417 majority of icosahedral nontailed phages observed had head sizes <70 nm, making it likely that

418 these could be bacteriophages (Hanson, Berges & Young, 2017).

419 In summer 2018, the proportion of viral particles with a capsid diameter <100 nm (mainly

420 bacteriophages) of N_{VF} (96%) is higher than in spring 2016 (80%); conversely, the proportion of

421 viruses with a capsid diameter >100 nm (hosts of which are mainly algae and other eukaryotic

422 organisms) is significantly lower in summer (4%) than in spring (20%). As a result, the average

423 capsid diameter of viruses in summer (51.7±1.3 nm, present study) was lower than in spring

424 (79.8±1.3 nm (Kopylov et al., 2019)). The presence of a large number of phycoviruses in Kara

425 Sea shelf waters in early spring 2016 was probably due to the end of the diatom bloom on the

426 lower surface of ice. This was evidenced by both the appearance of the lower edge of the ice,

427 colored brown, and the remains of characteristic colonies of ice algae (mainly *Nitzshia frigida*

428 Grunow, 1880) in surface water samples. In addition, during this period, the bloom of

429 *Phaeocystis pouchetii* (Hariot) Lagerheim, 1896 had begun, already forming numerous colonies

430 (Sazhin et al., 2017).

431

432 **Viral infection and virus-mediated mortality of prokaryotes**

433

434 In Arctic waters, the *FVIC* and *VMPR* values most often vary from 0.5% of N_{PR} and 3.7% of P_{PR}

435 (central Arctic region (Steward et al., 2007)) to 2.1% N_{PR} and 20.2% of P_{PR} (coastal waters of the

436 Novaya Zemlya archipelago (Venger et al., 2016)). Thus, in summer, the average *FVIC* and

437 *VMPR* values in surface waters on the Kara Sea shelf are in the middle of the range of values

438 determined in different regions of the Arctic (Steward, Smith & Azam, 1996; Middelboe,

439 Nielsen & Bjørnsen, 2002; Boras et al., 2010).

440 As is known, the frequency of contacts between viral particles and prokaryotic cells depends on

441 their respective abundance, the physical and chemical parameters of the water, and the size of a

442 given prokaryotic cell and given viral capsid (Murray & Jackson, 1992). It is possible that the

443 relatively larger size of rods and vibrios (from 0.6×0.2 to 1.7×0.6 µm) and filamentous

444 prokaryotes (from 1.1×0.3 to 2.7×0.8 µm) compared to the cocci and ellipsoids cell (from 0.3

445 $\times 0.2$ to 1.0×0.6 µm) contributes to a higher frequency of contacts between these morphological

446 types of prokaryotes and viruses and, as a consequence, to the higher probability of viral

447 infection of these prokaryotes.

448 A high concentration of *PD* with less than 4 µm in size was found in surface waters of the Kara

449 Sea shelf; their abundance exceeded that of prokaryotes. A large amount of *PD* with attached

450 viruses was detected. The average abundance of viruses attached to pico-sized *PD* exceeded

451 fivefold the average abundance of viruses attached to prokaryotes, suggesting that adsorption of

452 viral particles to pico-sized *PD* reduced both the abundance of free viruses and the level of viral

453 infection of prokaryotes. A negative correlation was found between the abundance of *PD* and

454 *FVIC* $r = -0.67$, $p = 0.0008$.

455 By adsorption to nonliving organic particles, the viruses are thus, at least temporarily,

456 unavailable for infection of new host cells, and adsorption of viruses to organic particles is

457 expected to have a profound inhibitory effect on virally mediated mortality of microorganisms

458 (Brussaard, Kuipers & Veldhuis, 2005; Mojica & Brussaard, 2014).

459 The low abundance of viruses during the transitional period from spring to summer is explained

460 by adsorption of viruses to suspended inorganic particles entering Arctic coastal waters with

461 runoff from adjacent land and to detrital particles formed in large quantities after the

462 phytoplankton bloom (Schoemann et al., 2005).

463   Recently, it was experimentally demonstrated that different virus populations strongly adsorb to

464   fine-grained glacial sediments. Moreover, production of progeny was strongly delayed in the

465   presence of glacial sediments (Maat, Prins & Brussaard, 2019; Maat, Visser & Brussaard, 2019).

466   In the CA, the abundance of prokaryotes was 6.3 times higher than in the MA. At the same time,

467   the abundance of free viruses in the CA was 1.4 times higher than in MA. A higher concentration

468   of suspended particles in waters of the eastern Kara Sea may be one of the possible reasons for

469   the relatively low concentration of free viruses in the CA, as well as in some other marine

470   habitats (Hewson & Fuhrman, 2003; Maat, Visser & Brussaard, 2019). According to our data,

471   the weight of detrital particles with a size of 0.254.0 μm on average for the area is three times

472   higher in the CA than in the MA. The lowest (0.2–0.5 mg L^{-1}) suspended particulate matter

473   (SPM, particle size from 0.47 to 1 mm) were detected in the western Kara Sea, whereas the

474   SPM concentration reaches 10 mg L^{-1} in the eastern part (Burenkov, Goldin & Kravchishina,

475   2010). Based on our data, the average abundance of viruses attached to detrital particles less than

476   4 μm in size were twice as high in the CA as in the MA. It was shown earlier that the low viral

477   abundance generally observed in the presence of high suspended particle load might be caused

478   by adsorption to suspended particles (Simon et al., 2002). We hypothesize that, higher

479   concentrations of suspended particles entering the CA in large amounts with Ob and Yenisei

480   runoff and, correspondingly, higher adsorption of viruses to these particles resulted in the

481   reduced abundance of free-living viruses and hence a lower specific contact rate between

482   prokaryotes and viruses, decreasing the frequency of visibly infected prokaryotic cells.

483

484   **CONCLUSIONS**

485

486   In late June–early July (i.e., at the end of the phenological spring–early summer), viruses are an

487   essential component of the planktonic microbial community on the Kara Sea shelf, averaging

488   about 10% of the prokaryotic biomass. The abundance of free viruses in very early summer was

489   higher than those found on the Kara Sea shelf in early spring and autumn. A strong positive

490   correlation was found between the abundance of prokaryotes and free viruses. Free viruses

491   significantly prevailed in the total abundance of virioplankton. Nontailed viruses quantitatively

492   constituted the majority of free viruses in Kara Sea water samples. The predominant viral

493   particles had a capsid diameter of 16–60 nm.

494   A large number of viruses were attached to detrital particles with a size of 0.25–4.0 μm. The

495   negative correlation between the frequency of virus-infected prokaryotic cells and the abundance

496   of pico-sized detrital particles suggests that the latter are an important factor reducing the level of

497   viral infection of prokaryotes. According to the obtained values of viral-mediated mortality of

498   prokaryotes, in early summer, viruses in general play an appreciable role in controlling the

499   abundance of prokaryotes on the Kara Sea shelf.

500

501   **ACKNOWLEDGEMENTS**

502

503   The authors would like to thank S.I. Metelev, G. Bykov, and Z. Bykova of the Centre for

504   Electron Microscopy, Papanin Institute for Biology of Inland Waters, Russian Academy of

505   Sciences, for their help in preparing material for electron microscopy. The authors are deeply

506   grateful to Dr. Aaron Carpenter for correcting the English translation. The authors are also

507   grateful to three anonymous reviewers for their thorough work with the manuscript.

508

509   **ADDITIONAL INFORMATION AND DECLARATIONS**

510

511   **Funding**

512   The research was supported by Russian Science Foundation project no. 22-17-00011.

513

514   **Grant Disclosures**: htpps://rscf.ru/project/22-17-00011.

515

516   **Competing Interests**

517

518   The authors declare that there are no competing interests.

519

520   **Author Contributions**

521   Alexander I. Kopylov conceived, designed, and performed experiments, wrote the paper,

522   prepared tables, and approved the final draft.

523   Elena A. Zabotkina conceived, designed, and performed experiments, analyzed data, prepared

524   figures, reviewed drafts of the paper, and approved the final draft.

525 Andrey F. Sazhin conceived, designed, and performed experiments, analyzed data, and approved

526 the final draft.

527 Nadezhda D. Romanova conceived, designed, and performed experiments, analyzed data, and

528 approved the final draft.

529 Anastasia M. Drozdova and Nicolay A. Belyaev performed experiments, analyzed data, and

530 approved the final draft.

531

532 **REFERENCES**

533

534 Alonso MC, Jimenez-Gomez F, Rodriguez J, Borrego JJ. 2001. Distribution of virus-like

535 particles in an oligotrophic marine environment (Alboran sea, Western Mediterranean).

536 *Microbial Ecology* 42: 407−415. DOI: 10.1007/s00248-001-0015-y.

537 Auguet JC, Montanié H, Delmas D, Hartmann HJ, Huet V. 2005. Dynamic virioplankton

538 abundance and its environmental control in the Charente estuary (France). *Microbial Ecology* 50:

539 337−349. https://doi.org/10.1007/s00248-005-0183-2.

540 Auguet JC, Montanie H, Lebaron P. 2006. Structure of virioplankton in the Charente Estuary

541 (france): transmission electron microscopy versus pulsed field gel electrophoresis. *Microbial*

542 *Ecology* 2006: 197−208. DOI: 10.1007/s00248-005-0043-0

543 Belyaev NA, Peresypkin VI, Ponyaev MS. 2010. The organic carbon in the water, the particulate

544 matter, and the upper layer of the bottom sediments of the west Kara Sea. *Oceanology* 50: 706–

545 715. https://doi.org/10.1134/S0001437010050085.

546 Bergh Ø, Borsheim KY, Bratbak G, Heldal M. 1989. High abundance of viruses found in aquatic

547 environments. *Nature* 340: 467−468. https://doi.org/10.1038/340467a0

548 Binder B. 1999. Reconsidering the relationship between virally induced bacterial mortality and

549 frequency of infected cells. *Aquatic Ecology* 18: 207−215. DOI: 10.3354 /AME018207.

550 Boras JA, Sala MM, Arrieta JM, Sa EL, Felipe J, Agustí S, Duarte CM, Vaqué D. 2010. Effect

551 of ice melting on bacterial carbon fluxes channeled by viruses and protists in the Arctic Ocean.

552 *Polar Biology* 33: 1695−1707. https://doi.org/10.1007/s00300-010-0798-8.

553 Bratbak G, Thingstad TF, Heldal M. 1994. Viruses and the microbial loop. *Microbial Ecology*

554 28: 209−221. https://doi.org/10.1007/BF00166811.

555 Brum JR, Schenck RO, Sullivan MB. 2013. Global morphological analysis of marine viruses

556 shows minimal regional variation and dominance of nontailed viruses. *The ISME Journal* 7:

557 1738−1751. doi:10.1038/ismej.2013.67

558 Brussaard CPD, Kuipers B, Veldhuis MJW. 2005. A mesocosm study of Phaeocystis globosa

559 population dynamics – I. Regulatory role viruses in bloom control. *Harmful Algae* 4: 859–874.

560 https://doi.org/10.1016/j.hal.2004.12.015.

561 Burenkov VT, Goldin YuA, Kravchishina MD. 2010. Distribution of suspended particulate

562 matter concentration in the Kara Sea in September 2007 based on wessel and satellite data.

563 *Oceanology* 50: 842–849. DOI:10.1134/S0001437010050164

564 Carstens EB. 2012. Introduction to Virus Taxonomy. In: King AMQ, Adams MJ, Carstens EB,

565 Lefkowitz EJ, eds. *Virus Taxonomy: Ninth Report of the International Committee on Taxonomy*

566 *of Viruses*. San Diego: Academic Press. 3–20. https://doi.org/10.1016/B978-0-12-384684-

567 6.00114-2

568 Clasen JL, Brigden SM, Payet JP, Suttle CA. 2008. Evidence that viral abundance across oceans

569 and lakes is driven by different biological factors. *Freshwater Biology* 53: 1090–1100.

570 https://doi.org/10.1111/j.1365-2427.2008.01992.x.

571 Cochlan WP, Wikner J, Steward GF, Smith DC, Azam F. 1993. Spatial distribution of viruses,

572 bacteria and chlorophyll a in neretic, oceanic and estuarine environments. *Marine Ecology*

573 *Progress Series* 92: 77−87. DOI: 10.3354/meps092077.

574 Guixa-Boixereu N, Vaqué D, Gasol JM, Sánchez-Cámara J, Pedrós-Alió C. 2002. Viral

575 distribution and activity in Antarctic waters. *Deep Sea Research II* 49: 827–845.

576 https://doi.org/10.1016/S0967-0645(01)00126-6.

577 Hammer Ø, Harper DA, Ryan PD. 2001. PAST: Paleontological statistics software package for

578 education and data analysis. *Palaeontologia electronica* 4(1) 4: 9.

579 Hanson AM, Berges JA, Young EB. 2017. Virus morphological diversity and relationship to

580 bacteria and chlorophyll across a freshwater trophic gradient in the Lake Michigan watershed.

581 *Hydrobiologia* 794: 93–108. https://doi.org/10.1007/s10750-016-3084-0

582 Hewson L, Fuhrman LA. 2003. Viriobenthos production and virioplankton sorptive scavenging

583 by suspended sediment particles in coastal and pelagic waters. *Microbial Ecology* 46: 337–347.

584 DOI: 10.1007/s00248-002-1041-0

585 Hodges LR, Bano N, Hollibaugh JT, Yager P. 2005. Illustrating the importance of particulate
586 organic matter to pelagic microbial abundance and community structure – an Arctic case study.
587 *Aquatic Microbial Ecology* 40: 217–227. DOI: 10.3354/ame040217.
588 Holmes RM. McClelland JM, Peterson BJ, Tank SE, Bulygina E, Eglinton TI, Gordeev VV,
589 Gurtovaya TY, Raymond PA, Repeta DJ et al. (2012) Estuaries and Coats 35: 369–382. DOI:
590 10.1007/s12237-011-9386-6
591 Kopylov AI, Zabotkina EA, Sazhin AF, Romanova ND. 2015. Virioplankton in the Kara Sea: the
592 impact of viruses on mortality of heterotrophic bacteria. *Oceanology* 55(4): 561–572.
593 https://doi.org/10.1134/S0001437015040104.
594 Kopylov AI, Zabotkina EA, Romanenko AV, Sazhin AF, Romanova ND. 2017. Virio- and
595 bacterioplankton in the estuary zone of the Ob River and adjacent regions of the Kara Sea shelf.
596 *Oceanology* 57(1):105–113. https://doi.org/10.1134/S0001437017010052.
597 Kopylov AI, Sazhin AF, Zabotkina EA, Romanenko AV, Romanova ND, Boltenkova MA. 2019.
598 Virioplankton of the Kara Sea and the Yenisei River estuary in early spring. *Estuarine, Coastal*
599 *and Shelf Science* 217: 37–44. https://doi.org/10.1016/j.ecss.2018.10.015.
600 Kopylov AI, Zabotkina EA, Sazhin AF, Kosolapov DB, Romanenko AV, Romanova ND. 2022.
601 Structure of virioplankton and viral lysis of prokaryotes on the shelf of Siberian Arctic seas:
602 impact of large river runoff. Polar Biology 45: 1581–1596. https://doi.org/10.1007/soo300-022-
603 03087-4.
604 Lasareva EV, Parfenova AM, Romankevich EA, Lobus NV, Drozdova AN. 2019. Organic
605 matter and mineral interections modulate flocculation across arctic river mixing zones. *JGR*
606 *Biogeosciences* 124: 1651–1664. https://doi.org/10.1029/2019jg005026.
607 Maat DS, Prins MA, Brussaard CPD. 2019. Sediments from Arctic tide-water glaciers remove
608 coastal marine viruses and delay host infection. *Viruses* 11(2): 123.
609 https://doi.org/10.3390/v11020123.
610 Maat DS, Visser RJW, Brussaard CPD. 2019. Virus removal by gracier-derived suspended fine
611 sediment in the Arctic. *Journal of Experimental Marine Biology and Ecology* 521: 151–227.
612 https://10.1016/j.jembe.2019.151227.
613 Makkaveev PN, Melnikova ZG, Polukhin AA, Stepanova SV, Khlebopashev PV, Chultsova AL.
614 2015. Hydrochemical characteristics of the waters in the western part of the Kara Sea.
615 *Oceanology* 55(4): 485−496. DOI: 10.1134/S0001437015040116.

616 Maranger R, Vaqué D, Nguyen D, Hébert MP, Lara E. 2015. Pan-Arctic patterns of planktonic

617 heterotrophic microbial abundance and processes: controlling factors and potential impacts of

618 warming. *Progress in Oceanography* 139: 221–232.

619 https://doi.org/10.1016/j.pocean.2015.07.006.

620 Middelboe M. 2000. Bacterial growth rate and marine virus-host dynamics. *Microbial Ecology*

621 40: 114–124. DOI: 10.1007/s002480000050

622 Middelboe M, Nielsen TG, Bjørnsen PK. 2002. Viral and bacterial production in the north water

623 in situ measurements batch-culture experiments and characterization of a viral-host system. *Deep*

624 *Sea Research Part II: Topical Studies in Oceanography* 49: 5063−5079.

625 https://doi.org/10.1016/S0967-0645(02)00178-9.

626 Mostajir B, Dolan J, Rassoulzadegan F. 1995. A simple method for the quantification of a class a

627 labile marine pico- and nano-sized detritus: DAPI Yellow Particles (DYP). *Aquatic Microbial*

628 *Ecology* 9: 259–266. https://doi.org/10.3354/ame009259.

629 Mojica KDA; Brussaard CPD. 2014. Factors affecting virus dynamics and microbial host-virus

630 interactions in marine environments. *FEMS Microbiology Ecology* 89: 495−515.

631 https://doi.org/10.1111/1574-6941.12343.

632 Murray AG, Jackson GA. 1992. Viral dynamics: a model of the effects of size, shape, motion

633 and abundance of single-celled planktonic organisms and other particles. *Marine Ecology*

634 *Progress Series* 89: 103–116. https://doi.org/10.3354/meps089103.

635 Noble RT, Fuhrman JA. 1998. Use of SYBR Green for rapid epifluorescence count of marine

636 viruses and bacteria. *Aquatic Microbial Ecology* 14: 113−118. DOI:10.3354/AME014113.

637 Norland S. 1993. The relationship between biomass and volume of bacteria. In: Kemp PF, Sherr

638 BF, Sherr EB, Cole JJ, eds. *Handbook of Methods in Aquatic Microbial Ecology* Boca Raton:

639 Lewis Publ. 303–308.

640 Porter KG, Feig YS. 1980. The use DAPI for identifying and counting of aquatic microflora.

641 *Limnology and Oceanography* 25(5): 943−948. https://doi.org/10.4319/lo.1980.25.5.0943.

642 Primpas I, Karydis M. 2011. Sealing the trophic index (TRIX) in oligotrophic marine

643 environments. *Environmental Monitoring and Assessment* 178: 257–269. DOI: 10.1007/s10661-

644 010-1687-x

645   Proctor LM, Okubo A, Fuhrman JA. 1993. Calibration estimates of phage-induced mortality in

646   marine bacteria: ultrastructural studies of marine bacteriophage development from one-step

647   growth experiments. *Microbial Ecology* 25: 161−182. https://doi.org/10.1007/BF00177193.

648   Romanova ND, Boltenkova MA. 2020. Seasonal variability of bacterioplankton of the Yenisei

649   Estuary. *Oceanology* 60(1): 74−82. DOI: 10.1134/S0001437020010191.

650   Romanova ND, Boltenkova MA, Polukhin AA, Bezzubova EM, Shchuka SA. 2022.

651   Heterotrophic bacteria of the Ob River Estuary during Groving season: Spatial and Temporal

652   variability. *Oceanology* 62: 369−378. https.//doi.org/10.1134/s000143/022030109.

653   Sazhin AF, Mosharov SA, Romanova ND, Belyaev NA, Khlebopashev PV, Pavlova MA,

654   Druzhkova EI, Flint MV, Kopylov AI, Zabotkina EA, Ishkulov DG, Makarevich PR, Pasternak

655   AF, Makkaveev PN, Drozdova AN. 2017. The plankton community of the Kara Sea in early

656   spring. *Oceanology* 57: 222–224. https://doi.org/10.1134/S0001437017010179.

657   Sandaa R-A, Storesund JE, Olesin E, Paulsen ML, Larsen A, Bratbak G, Ray JL. 2018.

658   Seasonality drives microbial community structure, shaping both eukaryotic and prokaryotic

659   host–viral relationships in an arctic marine ecosystem. *Viruses* 10: 715.

660   https://doi.org/10.3390/v10120715.

661   Schoemann V, Becquevort S, Stefels J, Rousseau W, Lancelot C. 2005. *Phaeocystis* blooms in

662   the global ocean and their controlling mechanisms: a review. *Journal of Sea Research* 53: 43–66.

663   https://doi.org/10.1016/j.seares.2004.01.008.

664   Simon M, Grossart HP, Schweitzer B, Ploug H. 2002. Microbial ecology of organic aggregates

665   in aquatic ecosystems. *Aquatic Microbial Ecology* 28: 175−211. DOI:10.3354/ame028175.

666   Steward GF, Fandino LB, Hollibaugh JT, Whitledged TE, Azam F. 2007. Microbial biomass and

667   viral infections of heterotrophic prokaryotes in the sub-surface layer of the Central Arctic Ocean.

668   *Deep Sea Research Part I: Oceanographic Research Papers* 54: 1744−1757.

669   https://doi.org/10.1016/j.dsr.2007.04.019.

670   Steward GF, Smith DC, Azam F. 1996. Abundance and production of bacteria and viruses in the

671   Bering and Chukchi Seas. *Marine Ecology Progress Series* 131: 287−300.

672   DOI:10.3354/meps131287.

673   Stopar D, Černe A, Žigman M, Poljšak-Prijately M, Turk V. 2003. Viral abundance and high

674   prorotion of lysogens suggests that viruses are important members of the microbial community

675   in the Gulf of Trieste. *Microbial Ecology* 46: 249–256. https://doi.org/10.1007/BF03036884

676   Suttle CA. 1993. Enumeration and isolation of virus. In: Kemp PF, Sherr BF, Sherr EB, Cole JJ,

677   eds. *Handbook of Methods in Aquatic Microbial Ecology* Boca Raton: Lewis Publ, 121−134.

678   Suttle CA. 2007. Marine viruses – major players in the global ecosystem. *Nature Reviews*

679   *Microbiology* 5: 801–812. https://doi.org/10.1038/nrmicro1750.

680   Van Etten JL, Lane LG, Meints RH. 1991. Viruses and virus like particles of eukaryotic algae.

681   *Microbiological Reviews* 55(4): 586−620. DOI:10.1128/MMBR.55.4.586-620.1991.

682   Venger MP, Kopylov AI, Zabotkina EA, Makarevich PR. 2016. The influence of viruses on

683   bacterioplankton of the offshore and coastal parts of the Barents Sea. *Russian Journal of Marine*

684   *Biology* 42(1): 26–35. https://doi.org/10.1134/S106307401601017X.

685   Wells LE, Deming JW. 2003. Abundance of Bacteria, the Cytophaga-Flavobacterium cluster and

686   Archaea in cold oligotrophic waters and nepheloid layers of the Northwest Passage, Canadian

687   Archipelago. *Aquatic Microbial Ecology* 31: 19−31. https://doi.org/10.3354/ame031019.

688   Wells LE, Deming JW. 2006a. Characterization of cold-active bacteriophage on two

689   psychrophilic marine hosts. *Aquatic Microbial Ecology* 45: 15–29. DOI:10.3354/ame045015.

690   Wells LE, Deming JW. 2006b. Significance of bacterivory and viral lysis in bottom waters of

691   Franklin Bay, Canadian Arctic, during winter. *Aquatic Microbial Ecology* 43: 209−221.

692   DOI:10.3354/ame043209.

693   Weinbauer MG, Brettar L, Höfle MG. 2003. Lysogeny and virus-induced mortality of

694   bacterioplankton in surface, deep, and anoxic marinewaters. *Limnology and Oceanography* 48:

695   1457−1465. https://doi.org/10.4319/lo.2003.48.4.1457.

696   Weinbauer MG, Peduzzi P. 1994. Frequency, size and distribution of bacteriophages in different

697   marine bacterial morphotypes. *Marine Ecology Progress Series* 108: 11–20.

698   DOI:10.3354/meps108011

699   Weinbauer MG, Rassoulzadegan F. 2004. Are viruses driving microbial diversification and

700   diversity? *Environmental Microbiology* 6: 1–11. https://doi.org/10.1046/j.1462-

701   2920.2003.00539.x.

702   Wilhelm SW, Suttle CA. 1999. Viruses and nutrient cycles in the sea. *Bioscience* 49: 781−788.

703   https://doi.org/10.2307/1313569.

704   Wommack KE, Colvell RR. 2000. Virioplankton: Viruses in Aquatic Ecosystems. *Microbiology*

705   *and Molecular Biology Reviews* 64: 69−114. https://doi.org/10.1080/19475721003743843.

706   Zhang R, Weinbauer MG, Peduzzi P (2021) Aquatic viruses and climate change. Current Issues

707   in Molecular Biology 41: 357-380. DOI: https://doi.org/10/21775/cimb.041.357

The physical and chemical properties of the sampling locations in the Barents Sea and the Kara Sea from June 29 to July 15, 2018

* ND - no data **detrital particles 0.25 to 4.0 µm in size *Alk*: Alkalinity, B_{PD}: Mass of detrital particles, *DOC*: Concentration of dissolved organic carbon, N_{PD}: Abundance of detrital particles, *S*: Salinity, *SIC*: Sea ice cover, *T*: Temperature

Stn. name	Longitude E°	Latitude N°	Date	SIC, %	T, °C	S, psu	Alk, mg-eq L⁻¹	NO_2+NO_3, µM	PO_4, µM	Si, µM	N_{PD}, 10^5 particles mL⁻¹	B_{PD}, mg L⁻¹	DOC, mg L⁻¹
Barents Sea													
1	56°29	70°18	29.06.2018	0	6.4	28.98	2.312	0.21	0.09	10.51	3.1	0.5	2.62
25	56°68	70°22	15.07.2018	0	8.9	29.70	ND*	1.59	0.06	14.16	3.9	0.7	2.92
Kara Strait													
2	58°15	70°50	29.06.2018	0	1.2	33.42	ND	0.95	0.07	0.06	6.1	1.1	1.42
Kara Sea, Marine Area													
3	60°08	70°83	29.06.2018	100	-0.7	27.12	1.789	1.56	0.10	1.76	5.9	0.9	1.39
4	62°50	70°87	29.06.2018	100	-1.0	26.93	1.781	3.03	0.14	2.89	10.2	1.0	2.34
5	64°30	70°92	29.06.2018	25	1.6	30.41	2.274	0.44	0.19	2.83	15.6	1.6	1.66
6	67°68	71°79	29.06.2018	0	2.1	31.92	2.228	0.07	0.20	1.64	17.3	1.7	2.11
7	68°46	73°02	30.06.2018	0	1.9	32.23	2.266	0.11	0.24	5.29	2.5	0.4	2.38
8	70°82	73°74	30.06.2018	0	1.4	30.22	2.001	4.35	0.52	35.99	8.3	1.3	3.94
21	67°85	72°14	14.07.2018	0	4.8	30.67	1.933	0.11	0.07	2.08	16.1	1.3	3.30
22	66°92	71°55	14.07.2018	0	2.5	32.00	1.758	0.06	0.10	2.33	7.7	0.7	2.13
23	64°08	71°01	14.07.2018	25	2.4	32.56	2.031	0.06	0.07	1.38	1.8	0.3	1.98

24	60º78	70º80	15.07.2018	25	1.5	32.80	ND	0.09	0.13	1.01	2.2	0.2	1.62
Kara Sea, Coastal Area.													
9	73º57	73º89	30.06.2018	0	3.9	15.48	1.47	5.91	1.01	62.48	10.8	2.5	7.93
10	76º06	73º88	30.06.2018	0	3.2	14.00	1.637	2.09	0.21	69.59	1.2	2.7	5.87
11	78º06	73º54	30.06.2018	0	5.1	4.90	1.342	3.87	0.46	90.23	8.0	2.5	11.46
12	80º13	73º00	01.07.2018	0	7.9	0.25	0.462	7.24	0.91	78.46	6.3	2.3	9.64
17	79º52	73º27	13.07.2018	0	7.1	2.17	0.644	0.35	0.20	73.49	20.5	2.5	9.48
18	78º14	73º68	13.07.2018	0	6.9	13.48	1.385	0.17	0.33	64.68	15.0	2.2	7.85
19	76º00	73º80	13.07.2018	0	4.0	11.06	1.289	7.95	0.37	92.62	17.5	2.5	9.36
20	73º11	73º79	14.07.2018	0	3.4	25.13	1.531	0.68	0.26	3.66	20.4	2.0	6.96

Chlorophyll *a* concentration, abundance, mean volume cell and biomass of prokaryotes in the surface water layer on the Barents Sea and Kara Sea

Chl *a*: Chlorophyll *a* concentration, N_{PR}: abundance of prokaryotes, V_{PR}: mean volume cell of prokaryotes, B_{PR}: biomass of prokaryotes

Stations	Chl a, μg L^{-1}	N_{PR}, 10^5 cells mL^{-1}	V_{PR}, μm^3	B_{PR}	
				mg m^{-3}	mg C m^{-3}
Barents Sea					
1	0.570	5.3	0.032	16.72	5.26
25	0.621	10.0	0.035	34.53	10.59
Kara Strait					
2	0.282	0.7	0.042	2.99	0.87
Kara Sea, Marine Area					
3	0.441	0.9	0.077	7.09	1.74
4	0.883	0.8	0.057	4.65	1.24
5	2.453	0.6	0.043	2.82	0.82
6	3.433	1.3	0.041	5.15	1.51
7	10.365	2.2	0.036	8.0	2.44
8	3.823	4.6	0.035	16.13	4.95
21	0.272	3.0	0.051	15.31	4.23
22	0.065	1.4	0.059	8.06	2.14
23	0.180	1.9	0.055	10.36	2.80
24	0.318	1.7	0.033	5.56	1.73
Kara Sea, Coastal Area					
9	8.742	7.4	0.021	15.79	5.59
10	9.688	8.3	0.038	31.32	9.39
11	2.617	8.4	0.033	27.66	8.63
12	2.961	25.3	0.036	90.95	27.68
17	4.418	11.8	0.037	43.26	13.07
18	3.756	18.7	0.036	66.21	20.34
19	6.722	7.7	0.034	26.08	8.07
20	1.534	3.5	0.045	15.57	4.45

Abundance of free viruses (N_{VF}), ratio of abundance of free viruses to abundance of prokaryotes (*VPR*), capsid diameter of free viruses (D_{VF})

Station	N_{VF}, 10^5 viruses mL^{-1}	VPR	D_{VF}, nm	
			Mean±SE	Min–max
Barents Sea				
1	37	7.0	38±1	18−76
25	36	3.7	53±2	16−155
Kara Strait				
2	21	29.4	48±3	17−196
Kara Sea, Marine Area				
3	53	57.2	52±2	23−106
4	63	77.0	64±3	26−177
5	47	73.0	61±3	16−155
6	37	29.4	54±2	21−129
7	68	30.7	49±3	26−304
8	66	14.6	47±1	16−80
21	74	24.7	50±2	16−205
22	40	28.9	42±2	16−133
23	10	5.2	57±2	21−155
24	50	29.8	50±2	16−155
Kara Sea, Coastal Area				
9	38	5.2	48±2	17−115
10	51	6.2	54±2	20−123
11	103	12.3	62±3	17−184
12	117	4.6	53±2	16−194
17	57	4.8	46±2	16−133
18	82	4.4	54±3	16−202
19	36	4.7	47±2	19−150
20	63	18.2	45±2	16−124

Simple (r_S, Spearman rank) correlation coeffcients between the abundances prokaryotes and viruses, the virus to prokaryotic ratio, frequency of visibly infected prokaryotic cells (*FVIC*) and environmental parameters for the whole data set

Only significant correlations are presented. Levels of significance * <0.05, ** < 0.01, *** < 0.001. N_{PR}: abundance of prokaryotes, N_{VF}: viral abundance, VPR: the virus to prokaryotic ratio, FVIC: frequency of visibly infected prokaryotic cells, T: temperature, S: salinity, Alk: alkalinity, Si: silicate concentration, N_{PD}: the abundance of detrital particles 0.25 to 4.0 μm in size, Chl *a*: chlorophyll *a* concentration, DOC: concentration of dissolved organic carbon, n=21

Parameter	N_{PR}	N_{VF}	VPR	FVIC
N_{PR}		0.63, **	-0.88***	
T	0.86***		-0.84***	
S	-0.73***	-0.45*		
Alk	-0.72***			
Si	0.83***			
N_{PD}				-0.74***
Chl a	0.48*			
DOC	0.87***	0.48*	-0.695**	

Characteristics of prokaryotes with attached viruses and viruses attached to prokaryotes

N_{PRV} – the abundance of prokaryotes with attached viruses, N_{PRV}/N_{PR} – proportion of prokaryotes with attached viruses of the total abundance of prokaryotes, N_{VPR}/N_{PRV} – abundance of viruses on the surface of a single prokaryotic cell, N_{VPR} – abundance of viruses attached to prokaryotes, D_{VPR} – average capsid diameter of viruses attached to prokaryotes

Station	N_{PRV}, 10^5 cells mL^{-1}	N_{PRV}/N_{PR}, %	N_{VPR}/N_{PRV}, viruses cell^{-1}	N_{VPR}, 10^5 viruses mL^{-1}	D_{VB}, nm	
					Mean±SE	min–max
Barents Sea						
1	1.0	18.20	1.5±0,9	1.5	50±1	29–74
25	1.2	12.50	1.2±0.5	1.5	62±1	46–93
Kara Strait						
2	1.4	19.38	1.6±1.3	2.2	50±1	24–68
Kara Sea, Marine Area						
3	0.2	23.5	1.5±0.8	0.3	60±3	22–90
4	0.2	26.9	1.4±1.2	0.3	78±1	65–101
5	0.2	30.5	1.5±0.8	0.3	62±1	47–79
6	0.3	22.9	1.5±0.7	0.4	63±1	36–89
7	0.7	32.6	1.9±1.4	1.4	70±2	41–139
8	1.0	20.9	1.5±1.0	1.4	56±2	22–77
21	0.7	22.3	1.7±1.2	1.1	66±2	43–97
22	0.3	24.7	1.6±1.1	0.5	45±2	27–97
23	0.2	10.9	1.7±1.3	0.4	47±1	31–63
24	0.4	26.5	1.5±0.8	0.7	65±1	42–92
Kara sea, Coastal Area						
9	2.1	28.1	1.6±1.1	3.4	88±2	55–120
10	1.6	19.0	1.4±0.8	2.2	64±2	39–113
11	2.2	26.3	1.3±0.6	2.9	71±3	25–147
12	10.3	40.7	1.5±0.7	15.4	69±4	27–169
17	3.3	27.9	1.4±0.6	4.6	50±1	36–66
18	5.2	27.9	1.6±1.0	8.3	58±2	37–96
19	1.6	21.2	1.3±0.5	2.1	61±2	32–110
20	0.7	20.8	1.5±0.7	1.1	49±1	32–67

Characteristics of detrital particles with attached viruses and viruses attached to detrital particles

N_{PDV} – the abundance of detrital particles with attached viruses, D_{PD} – the diameter of detrital particles, N_{VPD}/N_{PDV} – the average number of viruses on a single particle, N_{VPD} – the abundance of viruses attached to detrital particles, D_{VPD} – the capsid diameter of a virus attached to particles

Station	N_{PDV}, 10^5 particles mL^{-1}	D_{PD}, µm		N_{VPD}/N_{PDV} viruses mL^{-1}	N_{VPD}, 10^5 viruses mL^{-1}	D_{VPD}, nm	
		min	max			Mean±SE	Min–max
Barents Sea							
1	1.5	0.25	3.0	2.1±1.5	3.2	48±1	30–67
25	1.0	0.45	3.5	1.1±0.5	1.1	25±1	25–45
Kara Strait							
2	2.0	0.25	4.0	2.6±1.3	5.2	55±2	39–84
Kara Sea, Marine Area							
3	1.9	0.5	4.0	1.9±1.4	3.6	72±2	35–87
4	0.7	0.3	3.0	1.4±0.6	1.0	55±2	41–81
5	2.9	0.3	2.5	1.8±1.2	5.2	45±1	26–71
6	4.0	0.3	2.5	2.0±1.4	8.0	56±2	33–79
7	1.0	0.3	4.0	2.4±1.7	2.4	69±2	36–88
8	0.9	0.5	4.0	3.2±1.7	2.9	69±4	40–137
21	2.8	0.5	1.5	2.0±1.5	5.6	47±1	25–59
22	2.0	0.25	2.0	2.4±1.7	4.8	67±2	44–111
23	0.8	0.25	4.0	2.2±1.9	1.8	51±2	21–85
24	0.9	0.3	2.5	2.4±1.7	2.2	55±1	38–76
Kara Sea, Coastal Area							
9	2.2	0.5	4.0	2.3±1.7	5.1	49±1	26–63
10	0.9	1.0	3.0	4.2±2.0	3.7	70±1	56–92
11	3.4	0.3	4.0	4.3±2.0	14.6	66±4	25–119
12	4.2	0.25	4.0	2.9±1.4	12.2	56±2	30–93
17	2.8	0.3	4.0	3.2±1.3	9.0	47±1	26–75
18	2.4	0.3	2.5	3.0±1.4	7.2	47±1	36–56
19	1.9	1.0	4.0	2.0±1.4	3.8	68±2	34–108
20	2.0	0.25	2.5	2.0±1.2	4.0	50±1	36–69

Frequency of visibly infected prokaryotes and infected prokaryotes, virus-mediated prokaryotic mortality, number of phages inside cells and ratio of the number of infected cells to the number of cells with attached viruses

FVIC – the frequency of visibly infected prokaryotic cells, FIC – the frequency of infected prokaryotic cells, VMB – the virus-mediated prokaryotic mortality, BS – the number of mature phages inside prokaryotic cells, N_{PRVIC}/N_{PRV} – the ratio of the abundance of infected cells to the abundance of cells with attached viruses, %

Station	$FVIC$, % от N_{PR}	FIC, % of N_{PR}	$VMPR$, % of P_{PR}	BS, viruses cell^{-1}		N_{PRVIC}/N_{PRV}, %
				Mean±SE	Max	
Barents Sea						
1	2.2	14.5	19.2	5.7±0.1	8	11
25	1.4	9.0	10.6	10.0±0.4	15	18
Kara Strait						
2	1.8	12.0	15.1	6.0±0.2	8	20
Kara Sea. Marine Area.						
3	1.9	12.7	16.1	7.0±0.2	11	17
4	1.3	8.8	10.4	6.0±0.2	9	28
5	1.4	9.0	10.6	6.0±0.3	11	28
6	0.4	2.8	2.9	4.0	4	147
7	3.5	22.1	34.0	5.0±0.2	9	14
8	1.2	8.2	9.5	5.8±0.3	10	26
21	0.8	5.5	6.1	6.0±0.2	8	56
22	0.8	5.5	6.1	6.3±0.1	8	40
23	1.2	8.2	9.5	17.0±0.7	24	30
24	1.2	8.2	9.5	5.5±0.1	7	42
Kara Sea. Coastal Area						
9	1.0	6.9	7.8	6.3±0.2	9	40
10	2.5	16.3	22.3	9.4±0.8	32	10
11	1.4	10.1	12.2	15.2±1.1	35	26
12	1.4	10.1	12.2	7.0±0.3	11	37
17	0.7	4.9	5.4	5.0±0.1	6	28
18	1.0	6.9	7.8	5.3±0.1	6	31
19	1.0	6.9	7.8	5.3±0.1	7	11
20	0.7	4.9	5.4	5.4	6	26

Figure 1

The scheme of the locations of the sampling stations.

● – circles denote stations samples were taken on June 29 - July 1, 2018; Δ – triangles denote stations samples were taken on July 12–15, 2018.
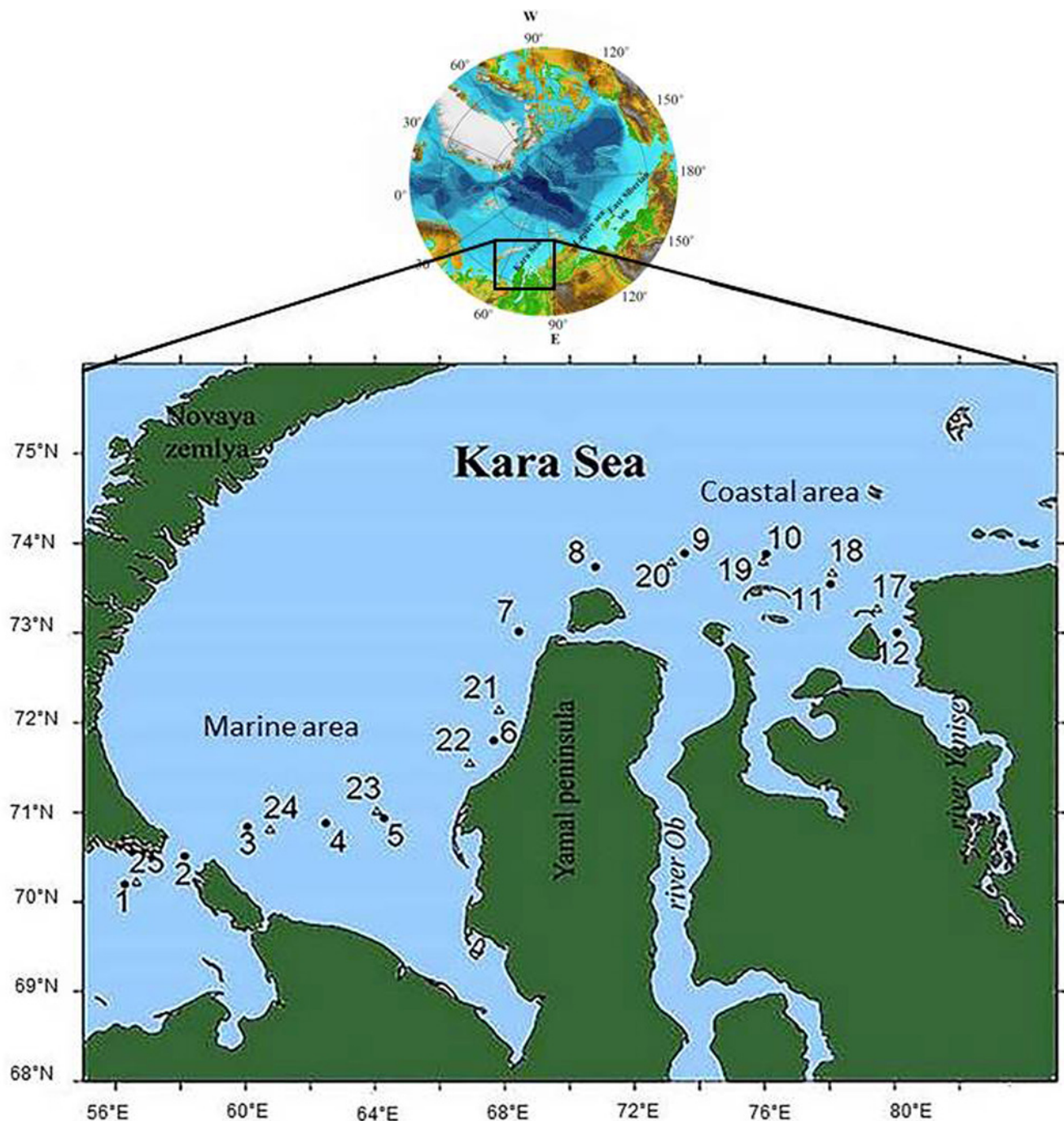
Figure 2

The average of primary physical and chemical parameters in different sections of the study area

Average (± standard error) of temperature, T (a); salinity, S (b); alkalinity, Alk (c); NO_2+NO_3 (d); PO_4 (e); silicate, Si (f); dissolved organic carbon, DOC (g); abundance of detrital particles 0.25 – 0.40 in size, N_{PD} (h); mass of of detrital particles 0.25 – 0.40 in size B_{PD} (i); in the surface water layer on the Barents and Kara seas.
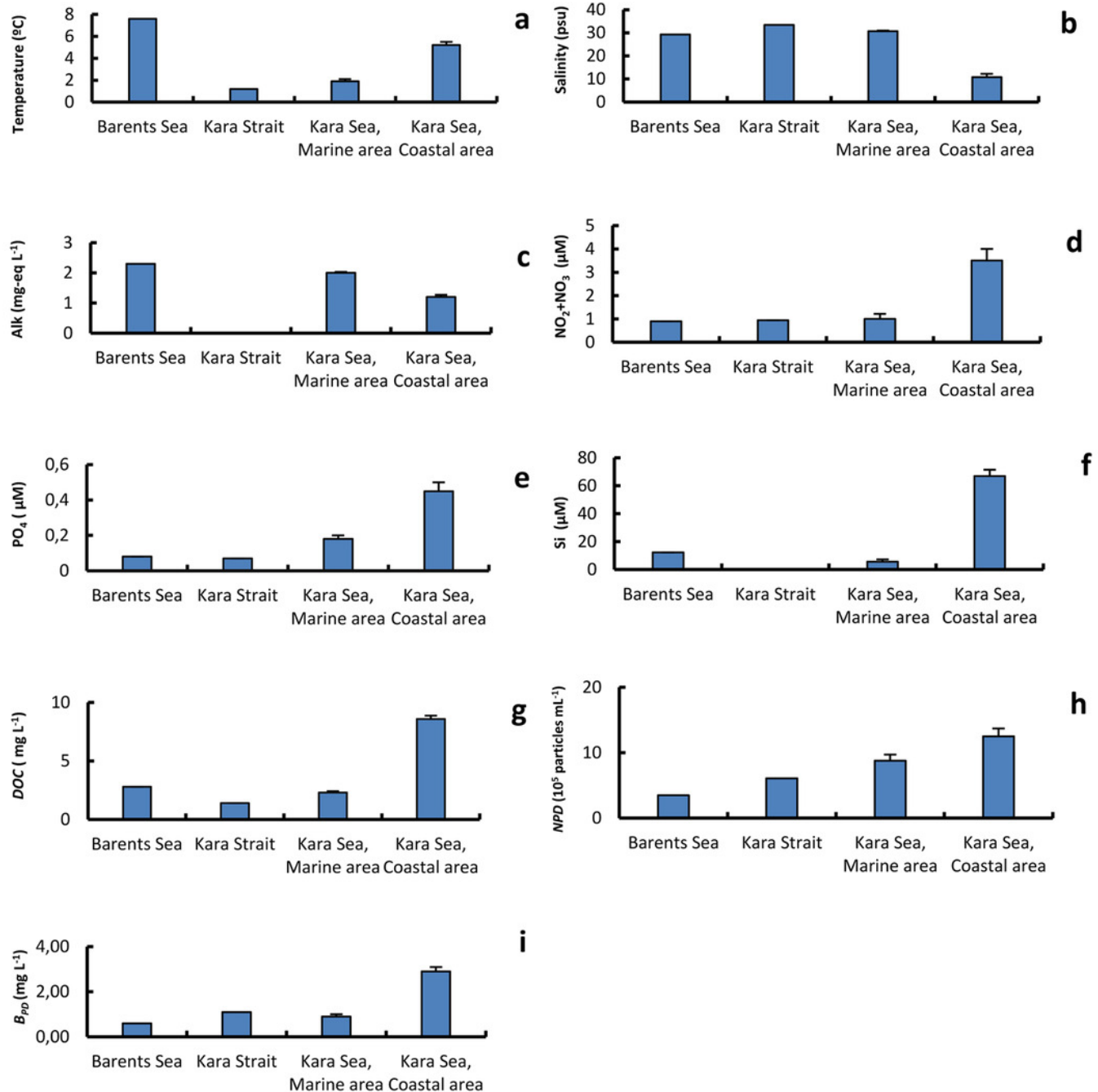
Figure 3

Electron micrographs of viruses in shelf waters of the Kara Sea. Examples of the four viral morphotypes: (a, b), myovirus; (c,d,e), podovirus; (f, g), siphovirus; (h,i), non-tailed virus; (j) prokaryote with viruses on surface, (k, l) virus-infected proka

Examples of the four viral morphotypes: (a, b), myovirus; (c,d,e), podovirus; (f, g), siphovirus; (h,i), non-tailed virus; (j) prokaryote with viruses on surface, (k, l) virus-infected prokaryote with viruses on surface, (m, n) viruses attached to detrital particles; (k, l) virus-infected prokaryotes − viruses inside cell observed in this study.
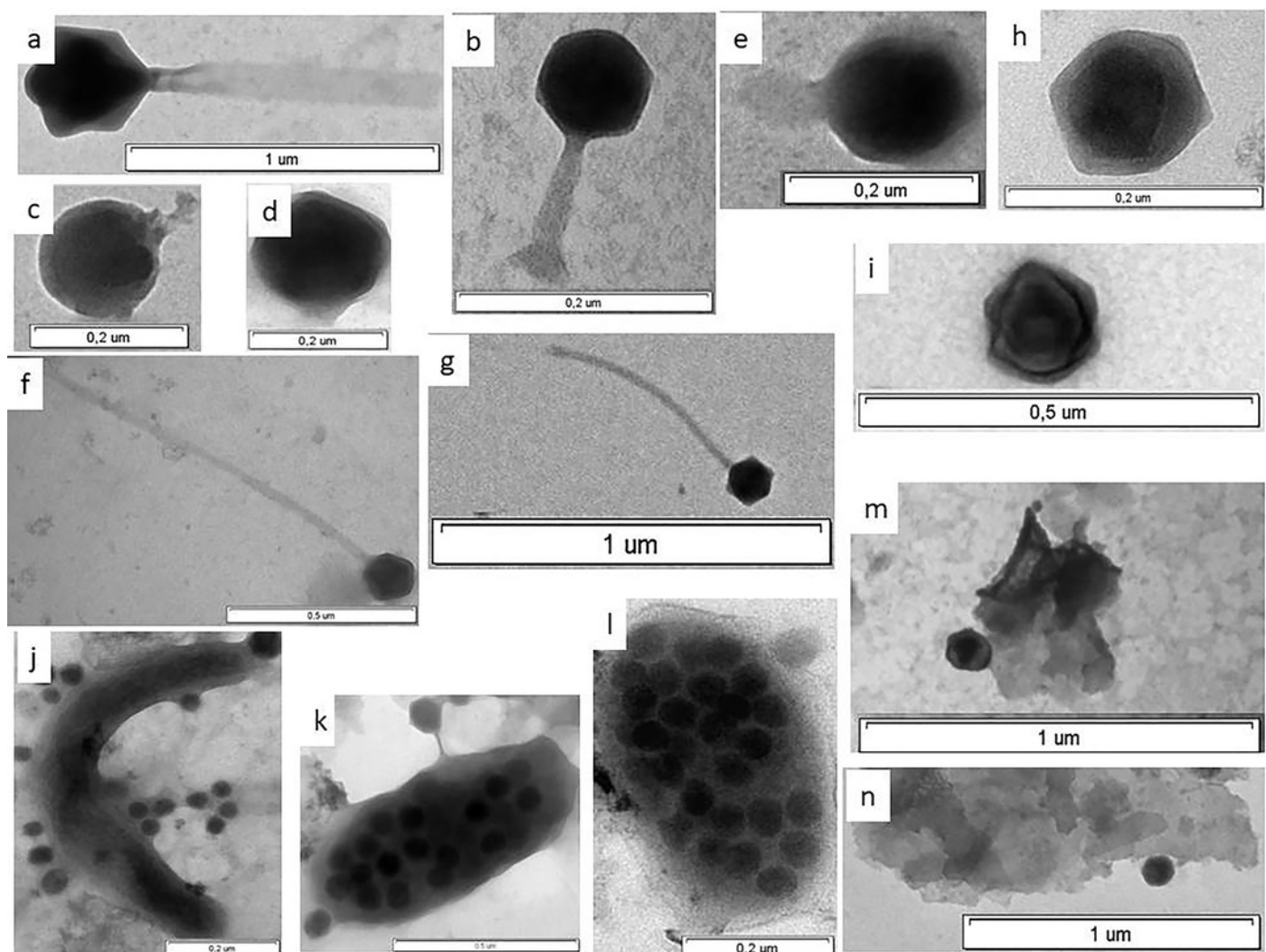
Figure 4

The average of primary biological parameters in different sections of the study area

Average (± standard error) of chlorophyll a, Chl a (a); abundance of prokaryotes, N_{PR} (b); abundance of free viruses, N_{VF} (c); ratio of abundance of free viruses to abundance of prokaryotes, VPR (d); abundance of viruses attached to prokaryotes, N_{VPR} (e), abundance of viruses attached to detrital particles, N_{VPD} (f), frequency of visibly infected prokaryotic cells, *FVIC* (g) in the surface water layer on the Barents and Kara seas.
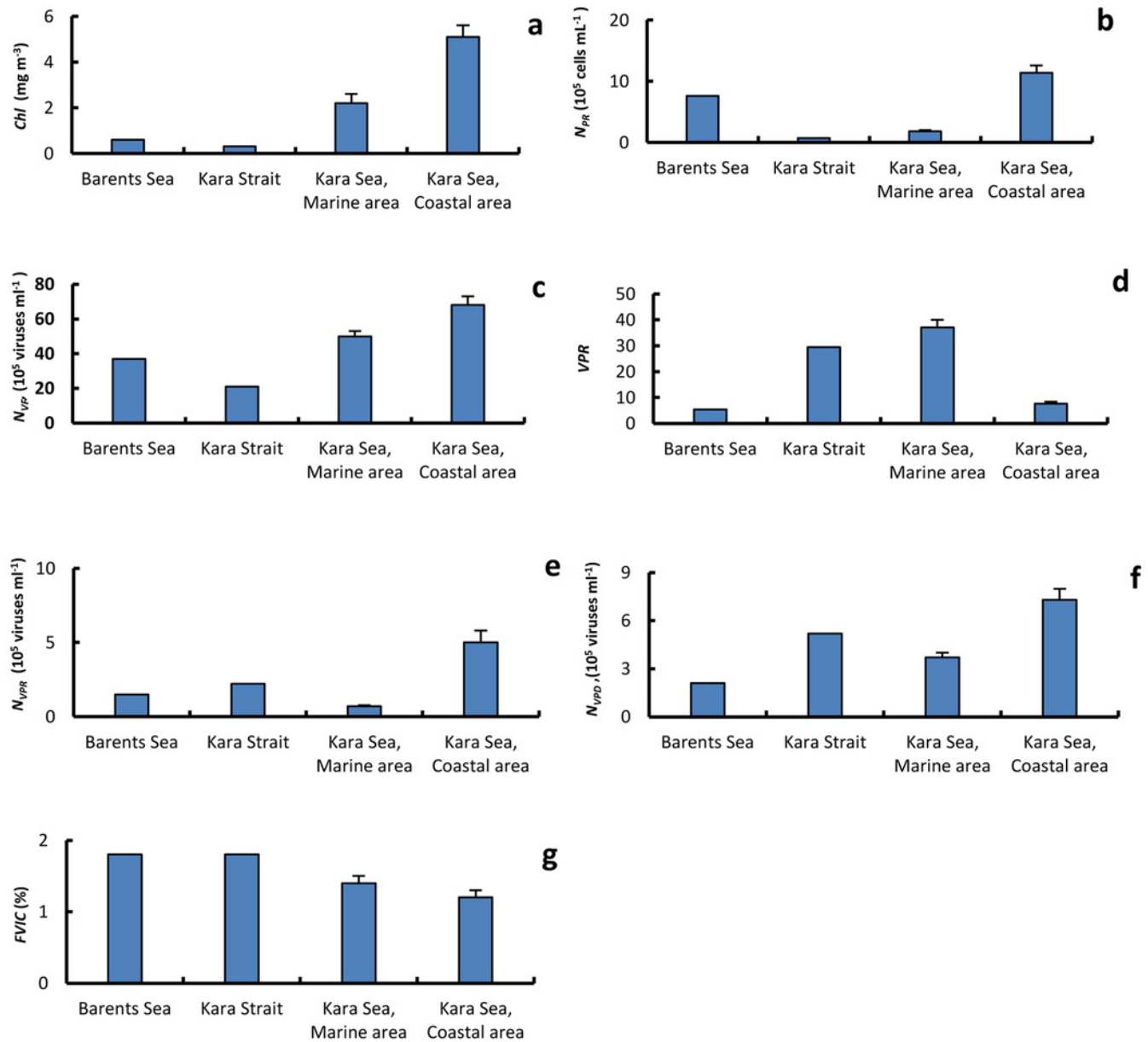
Figure 5

Percentage (mean ± standard error) of viral morphotypes in viral assemblages in the surface water layer of the Barents and Kara seas.
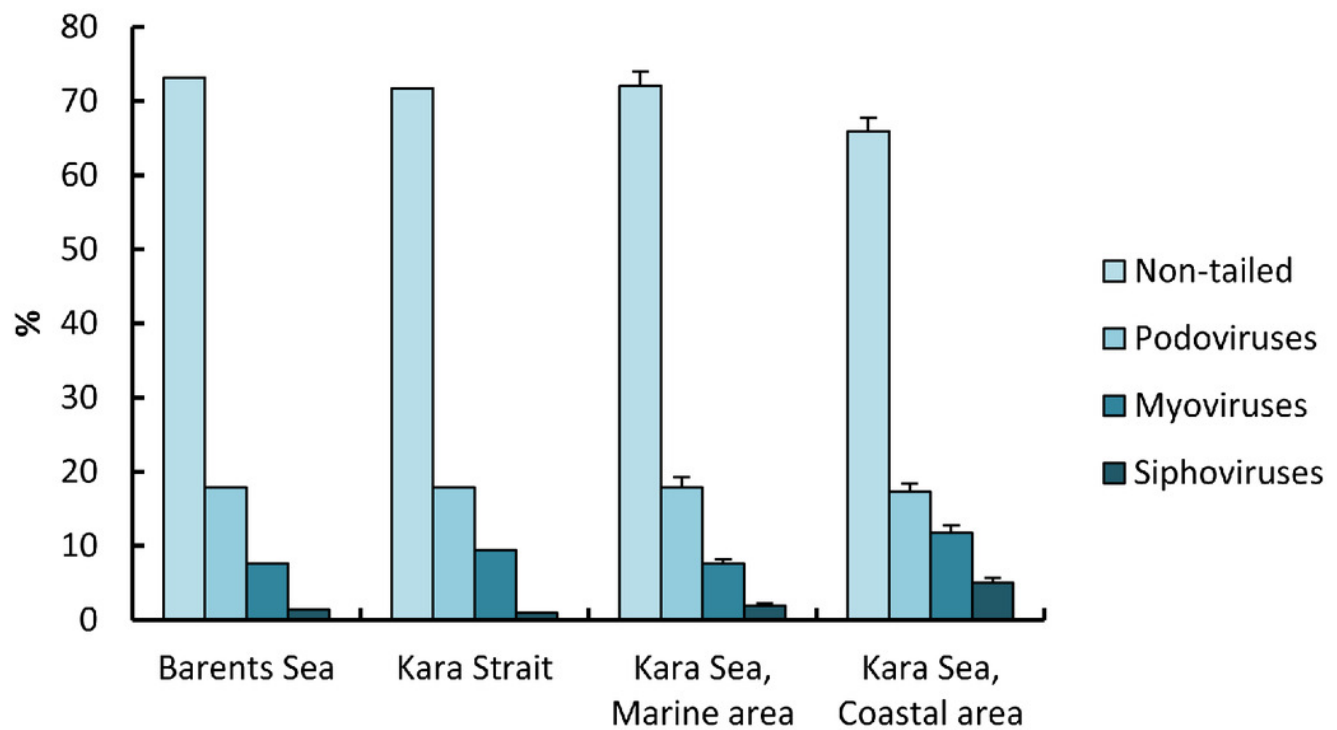
Figure 6

Proportions of prokaryotic cells of different morphology in the total number of prokaryotes and in the total number of infected cells

Percentage (%) of prokaryote cells of various morphology to the total prokaryote abundance (*a*); Percentage (%) of infected prokaryote cells of various morphology to the total number of infected prokaryote cells (*b*), Percentage (%) of infected prokaryote cells of various morphology to the number of prokaryote cells of a given type (*c*).

■ cocci and ellipsoids   ☐ rods and vibrios   ☐ filaments